Neuro-Oncology
23(12), 2042–2053, 2021 | doi:10.1093/neuonc/noab133 | Advance Access date 29 May 2021

Heterogeneous delivery across the blood-brain barrier limits the efficacy of an EGFR-targeting antibody drug conjugate in glioblastoma

Bianca-Maria Marin†, Kendra A. Porath†, Sonia Jain†, Minjee Kim, Jason E. Conage-Pough, Ju-Hee Oh, Caitlyn L. Miller, Surabhi Talele, Gaspar J. Kitange, Shulan Tian, Danielle M. Burgenske, Ann C. Mladek, Shiv K. Gupta, Paul A. Decker, Madison H. McMinn, Sylwia A. Stopka, Michael S. Regan, Lihong He, Brett L. Carlson, Katrina Bakken, Terence C. Burns, Ian F. Parney, Caterina Giannini, Nathalie Y. R. Agar, Jeanette E. Eckel-Passow, Jennifer R. Cochran, William F. Elmquist, Rachael A. Vaubel, Forest M. White, and Jann N. Sarkaria

Department of Radiation Oncology, Mayo Clinic, Rochester, Minnesota, USA (B.-M.M., K.A.P., S.J., G.J.K., D.M.B., A.C.M., S.K.G., L.H., B.L.C., K.B., J.N.S.); Department of Pharmaceutics, University of Minnesota, Minneapolis, Minnesota, USA (M.K., J.-H.O., Su.T., W.F.E.); Department of Biological Engineering, Massachusetts Institute of Technology, Cambridge, Massachusetts, USA (J.E.C.-P., F.M.W.); David H. Koch Institute for Integrative Cancer Research, Massachusetts Institute of Technology, Cambridge, Massachusetts, USA (J.E.C.-P., F.M.W.); Center for Precision Cancer Medicine, Massachusetts Institute of Technology, Cambridge, Massachusetts, USA (J.E.C.-P., F.M.W.); Department of Bioengineering, Stanford University, Stanford, California, USA (C.L.M., J.R.C.); Department of Biomedical Statistics and Informatics, Mayo Clinic, Rochester, Minnesota, USA (Sh.T., P.A.D., J.E.E.-P.); Department of Neurosurgery, Brigham and Women's Hospital, Harvard Medical School, Boston, Massachusetts, USA (M.H.M., S.A.S., M.S.R., N.Y.R.A.); Department of Chemistry and Chemical Biology, Northeastern University, Boston, Massachusetts, USA (M.H.M.); Department of Radiology, Brigham and Women's Hospital, Harvard Medical School, Boston, Massachusetts, USA (S.A.S., N.Y.R.A.); Department of Neurosurgery, Mayo Clinic, Rochester, Minnesota, USA (T.C.B., I.F.P.); Department of Laboratory Medicine and Pathology; Mayo Clinic, Rochester, Minnesota, USA (C.G., R.A.V.); Department of Cancer Biology, Dana-Farber Cancer Institute, Boston, Massachusetts, USA (N.Y.R.A.)

†Authors contributed equally to this work.

Corresponding Author: Jann N. Sarkaria, MD, Department of Radiation Oncology, Mayo Clinic, 200 First Street SW, Mayo Clinic, Rochester, MN 55902, USA (sarkaria.jann@mayo.edu).

Abstract

Background. Antibody drug conjugates (ADCs) targeting the epidermal growth factor receptor (EGFR), such as depatuxizumab mafodotin (Depatux-M), is a promising therapeutic strategy for glioblastoma (GBM) but recent clinical trials did not demonstrate a survival benefit. Understanding the mechanisms of failure for this promising strategy is critically important.

Methods. PDX models were employed to study efficacy of systemic vs intracranial delivery of Depatux-M. Immunofluorescence and MALDI-MSI were performed to detect drug levels in the brain. EGFR levels and compensatory pathways were studied using quantitative flow cytometry, Western blots, RNAseq, FISH, and phosphoproteomics.

Results. Systemic delivery of Depatux-M was highly effective in nine of 10 EGFR-amplified heterotopic PDXs with survival extending beyond one year in eight PDXs. Acquired resistance in two PDXs (GBM12 and GBM46) was driven by suppression of EGFR expression or emergence of a novel short-variant of EGFR lacking the epitope for the Depatux-M antibody. In contrast to the profound benefit observed in heterotopic tumors, only two of seven intrinsically sensitive PDXs were responsive to Depatux-M as intracranial tumors. Poor efficacy in orthotopic PDXs was associated with limited and heterogeneous distribution of Depatux-M into tumor tissues, and artificial

disruption of the BBB or bypass of the BBB by direct intracranial injection of Depatux-M into orthotopic tumors markedly enhanced the efficacy of drug treatment.

Conclusions. Despite profound intrinsic sensitivity to Depatux-M, limited drug delivery into brain tumor may have been a key contributor to lack of efficacy in recently failed clinical trials.

Key Points

1. EGFR-targeting ADC, Depatux-M is a promising therapy for GBM.
2. EGFR variants can drive resistance to Depatux-M.
3. ADC efficacy is limited by heterogeneous distribution across BBB.

Importance of the Study

ADCs targeting EGFR, like Depatux-M, are a promising therapeutic strategy for GBM but failed to provide a survival benefit in Intellance-I and Intellance-II clinical trials for patients with recurrent disease or newly diagnosed disease, and understanding the mechanisms of failure is critically important. In this study, Depatux-M was found to be highly effective in nine of 10 EGFR-amplified PDXs with >1-year survival in eight PDXs. In contrast, only two of seven sensitive PDXs were responsive to Depatux-M as intracranial tumors, and VEGF expression or intracranial drug injection markedly enhanced the drug efficacy. Acquired resistance in GBM12 and GBM46 was linked to reduced EGFR expression, a novel EGFR variant lacking the Depatux-M binding epitope, and enhanced compensatory signaling pathways. These studies provide insight into at least two failure mechanisms that may be contributory in the negative clinical trials.

Epidermal Growth Factor Receptor (EGFR) is a driver of gliomagenesis in almost half of glioblastomas (GBMs), and there has been tremendous effort focused on developing EGFR-targeting therapeutics for GBM.[1] Unfortunately, the efficacy of small molecule inhibitors and monoclonal antibodies that block EGFR signaling are limited by compensatory signaling pathways and molecular heterogeneity.[2] In contrast to these approaches that rely on robust suppression of signaling, EGFR-specific antibody drug conjugates (ADCs) use high-level cell surface expression of EGFR and subsequent internalization as a vehicle to deliver highly potent toxins to tumor cells while sparing normal tissues.

Depatuxizumab mafodotin (Depatux-M; ABT-414) is the most clinically advanced ADC being tested in humans. Depatux-M is composed of an EGFR-targeting antibody (ABT-806) conjugated to monomethyl auristatin F (MMAF) via a maleimidocaproyl (mc) noncleavable linker.[3] ABT-806 recognizes a unique epitope in the extracellular domain of EGFR, which is only accessible in the context of oncogenic EGFR signaling associated with overexpressed wild-type or exon-variant EGFR molecules.[4,5] Following internalization, catabolism of EGFR-bound Depatux-M in the lysosome releases cysteine-mc-MMAF (Cys-mc-MMAF), which binds to and inhibits microtubule polymerization.[6] While early trials were promising,[7] Phase III trials of Depatux-M combined with standard therapy did not provide a significant survival advantage in newly diagnosed or recurrent GBM.[8] Given the strong rationale and promising preclinical and early clinical results, understanding why this clinical strategy failed is of paramount importance.

This preclinical trial tested the efficacy of Depatux-M in 13 GBM patient-derived xenografts (PDXs) with varying EGFR characteristics. While the majority of EGFR-amplified PDXs were intrinsically sensitive to Depatux-M, treatment efficacy for intracranial tumors was limited by inadequate drug-delivery across an intact blood-brain barrier (BBB). Our data provide strong evidence that heterogeneous distribution across the BBB limits the clinical efficacy of ADCs in GBM.

Materials and Methods

Animal Studies

The Mayo GBM PDXs have been extensively described.[9,10] All animal studies were approved by the Mayo Institutional Animal Care and Use Committee. Subcutaneous tumors were established in athymic mice (Envigo), and tumor size was measured thrice weekly. Mice were randomized and treated with an isotype control antibody AB095 (10 mg/kg), ABT-806 (10 mg/kg), AB095-MMAF (5 mg/kg), or Depatux-M (5 mg/kg) intraperitoneally once a week for up to six months. Individual mice were euthanized after tumors exceeded 1500 mm^3. Where indicated, recurrent tumors were fresh-frozen, cryopreserved or used for cell culture.

Orthotopic tumors were established as described previously.[10] Tumor growth was monitored using bioluminescence imaging (BLI). Mice were stratified by BLI signal, randomized into groups, and treated with AB095 (5 mg/kg) or Depatux-M (5 mg/kg) intraperitoneally once a week. For intracranial dosing, mice were treated weekly with 10 µL of 10 mg/mL of AB095 or Depatux-M for a total of 4 doses starting 7 days post tumor injection. Mice were euthanized upon reaching a moribund state.

Statistical Analysis

Cumulative survival probabilities were estimated using the Kaplan–Meier method. Time was calculated from initial injection to date of death or last observation. Survival was compared across groups using the Log-Rank test. Analysis of variance, Kruskal–Wallis or Mann–Whitney tests as appropriate were used to make comparisons across groups. *P*-values <.05 were considered statistically significant.

Additional methods are in Supplementary Material.

Results

Intrinsic Sensitivity of GBM PDXs to Depatux-M

The Mayo Clinic has developed a panel of over 100 GBM PDXs.[9] The *in vitro* sensitivity to Depatux-M was evaluated across a subset of 10 EGFR-amplified PDXs and 3 EGFR nonamplified PDXs, selected based on WES[9] and EGFR protein expression (Figure 1A). The *in vitro* sensitivity to Depatux-M was compared to EGFR receptor cell surface density (Figure 1B, Supplementary Figure 1). All five EGFRvIII amplified PDXs expressed high level EGFR (6×10^5–8×10^6 receptors per cell) and were highly sensitive to Depatux-M *in vitro* with a 50% effective concentration (EC_{50}) ranging from 0.2 to 50 ng/ml, which was significantly more sensitive than other lines ($P = .004$) (Figure 1B). Conversely, the EGFR nonamplified PDXs (GBM10, GBM22, GBM43) had the lowest EGFR density (~1×10^4 per cell) and about 1000-fold higher EC_{50} (3–13 µg/ml) compared to EGFRvIII amplified lines ($P = .025$). The other EGFR amplified PDXs had intermediate EGFR expression (9×10^4–8×10^5 per cell), but their sensitivity to Depatux-M (EC_{50}: 5–15 µg/ml) was not significantly different than nonamplified lines ($P = .29$). GBM26 (A289T point mutant) did not grow well in culture so *in vitro* testing was not possible. Overall, the *in vitro* cytotoxicity assay identified EGFRvIII PDXs as the most sensitive to Depatux-M in comparison to other EGFR variants or nonamplified PDXs.

The intrinsic sensitivity of the 13 PDXs to Depatux-M was evaluated *in vivo* in heterotopic tumors. EGFR expression in PDX was confirmed retrospectively by immunoblotting recurrent AB095-treated tumors. There was a high concordance of EGFR expression by Western blotting, IHC, and WES analyses, except for GBM8. WES analysis of GBM8 predicted full-length EGFR expression, while an EGFR-immuno-reactive band was observed at both the EGFR full-length and EGFRvIII molecular weights, which could represent a nonglycosylated form of EGFR[11] or altered mRNA splicing to produce a truncated EGFR protein (Figure 1C). Strikingly, nine of 10 EGFR-amplified models had marked extension in survival with Depatux-M treatment; five PDXs, GBM6, GBM8, GBM26, GBM39, and GBM108 were exquisitely sensitive with more than 250-day prolongation in median time to regrowth following Depatux-M therapy compared to control (Figure 1D and Supplementary Table 1). In contrast, all three nonamplified PDXs (GBM10, GBM22, and GBM43) were highly resistant to therapy. Notably, three EGFR-amplified PDXs, GBM59, GBM12, and GBM46, exhibited a marked discordance between *in vitro* and *in vivo* sensitivity (Figure 1B and D). EGFRvIII amplified GBM59 was sensitive to Depatux-M (~5 ng/ml EC_{50}) *in vitro* but was highly resistant as a flank tumor. Conversely, GBM12 and GBM46 had relatively high EC_{50} (~5 µg/ml) *in vitro* but exhibited significant tumor control *in vivo* with prolonged tumor stasis prior to recurrence. Overall, the majority of EGFR-amplified PDXs are profoundly sensitive to Depatux-M.

Evaluation of Recurrent Flank Tumors Following Depatux-M Therapy

Three EGFR-amplified PDXs recurred during weekly Depatux-M therapy and represent models of acquired (GBM12 and GBM46) or inherent (GBM59) resistance (Figure 2A, Supplementary Figure 2A and C). Since cytotoxicity is critically linked to ADC internalization, the efficiency of ADC uptake was evaluated *in vitro* using live cell imaging. Interestingly, Depatux-M uptake for GBM59 was comparable to sensitive GBM6 and GBM39, while GBM12 and GBM46 exhibited more limited or nonspecific uptake of both AB095 and Depatux-M (Supplementary Figure 2E). GBM59 sensitivity to unconjugated MMAE toxin was similar to GBM6 sensitivity. Cytotoxicity of Depatux-M in GBM59 did not change with concurrent inhibition of multi-drug resistance-1 (MDR1) and breast cancer resistance protein 1 (BCRP1) mediated efflux using elacridar (Supplementary Figure 2F), and MDR1 expression was not detectable in GBM59 by Western blot (Supplementary Figure 2G). Mechanisms of resistance in these PDXs were further evaluated in recurrent flank tumor specimens from the efficacy studies. The regrowth of individual tumors was relatively similar within a given PDX (Figure 2A, Supplementary Figure 2A and C). Subsequent Western blotting of Depatux-M-recurrent tumors, compared to AB095-recurrent tumors, demonstrated near uniform suppression of EGFR expression in GBM12 and GBM46, while EGFR expression remained unchanged in GBM59 (Figure 2B and Supplementary Figure 2B and D). This observation suggests GBM12 and GBM46 acquired resistance during Depatux-M treatment by modulating expression of EGFR.

The Depatux-M resistant GBM12 PDX derived from animal #2802 (GBM12R-#2802) also exhibited emergence of an EGFR-immunoreactive band at approximately ~85 kDa (short-variant) in addition to full-length EGFR protein (Figure 2B). To study whether this EGFR variant was associated with resistance, two of the GBM12R (#2802, #5931) sublines were serially passaged. Passage of the GBM12R-#2802 tumor without Depatux-M selective pressure resulted in loss of the short-variant EGFR and re-emergence of the full-length EGFR (Supplementary Figure

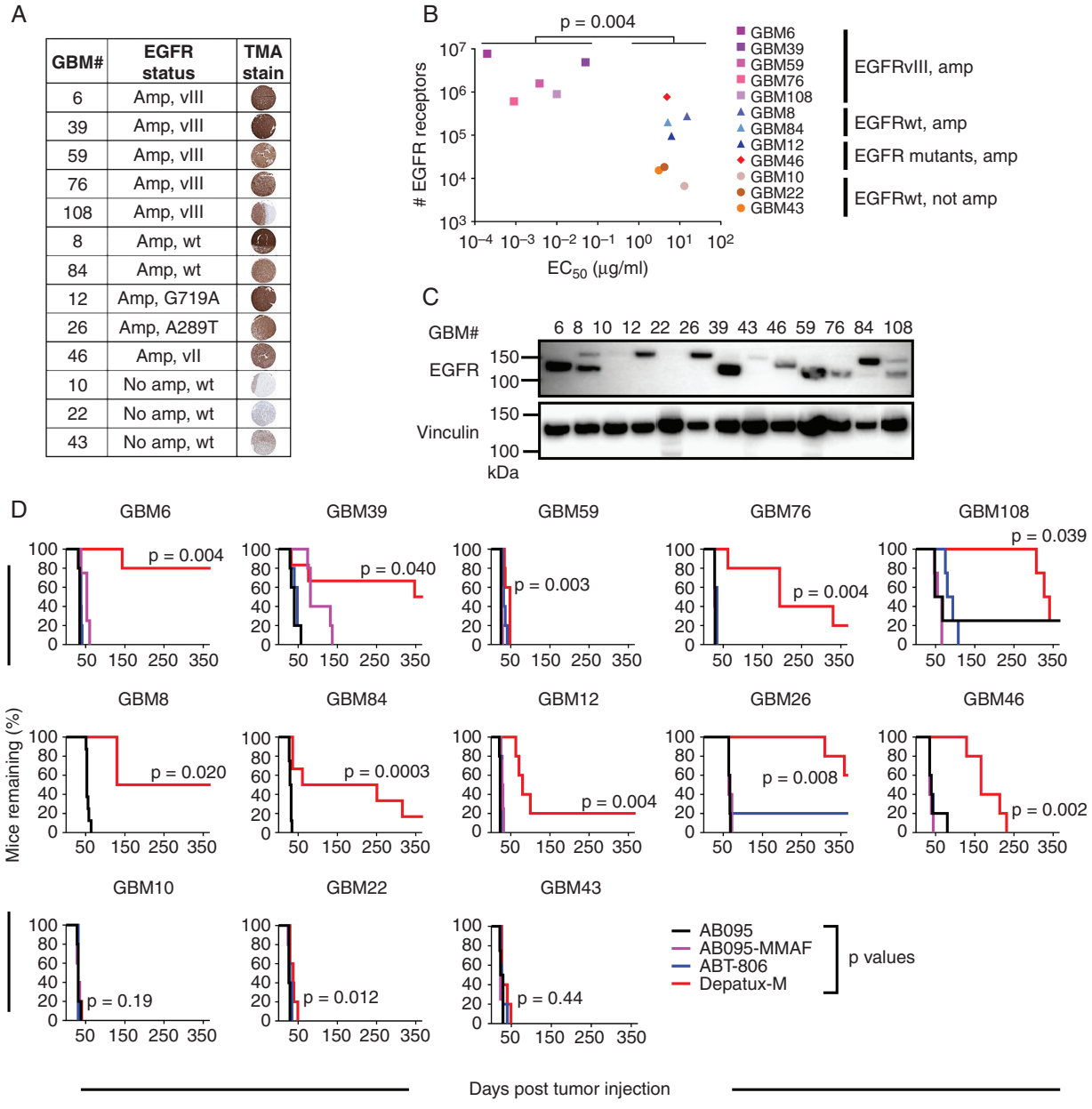

Fig. 1 Depatux-M therapy induces a spectrum of *in vitro* and *in vivo* responses in GBM PDXs. (A) EGFR characteristics of the 13 PDXs selected for the preclinical studies, determined by WES and TMA analysis. Representative EGFR stained sections are shown for each line. (B) Depatux-M *in vitro* potency (EC_{50}), determined using Cell Titer Glo cytotoxicity assay in relation to the number of EGFR molecules expressed on the cell surface, measured by quantitative flow cytometry using ABT-806. Significance between the EC_{50} of EGFRvIII expressing PDXs vs other PDXs is shown using Kruskal–Wallis test. (C) EGFR expression in pooled lysates from three AB095 treated tumors of each PDX line. Vinculin was used as a loading control. (D) Kaplan–Meier plots of 13 PDXs grown as flank tumors and treated with intraperitoneal injection of AB095 (nonspecific IgG; 10 mg/kg), AB095-MMAF (nonspecific ADC; 5 mg/kg), ABT-806 (ADC backbone without toxin; 10 mg/kg) or Depatux-M (ADC; 5 mg/kg). All groups were dosed with once weekly injections for 6 months or until euthanasia. X-axis depicts time to reach moribund state or euthanasia criteria. GBM10, GBM46 and GBM76 were derived from recurrent GBM samples, while the other 10 PDXs were derived from previously untreated GBM samples. Significance of endpoint comparison between Depatux-M and AB095 group is shown using Log-Rank test.

3A). In a subsequent therapy study comparing AB095 to Depatux-M, GBM12R-#2802 tumors did not regress with Depatux-M treatment but slowed tumor growth with a variable but significant prolongation of tumor regrowth, consistent with maintenance of resistance with serial passage (Figure 2C). Similar Depatux-M resistance was seen with GBM12R-#5931 tumors (Supplementary Figure 3B). Western blot analysis from both GBM12R sublines again demonstrated suppression of full-length EGFR expression and robust expression of a short-variant EGFR in some,

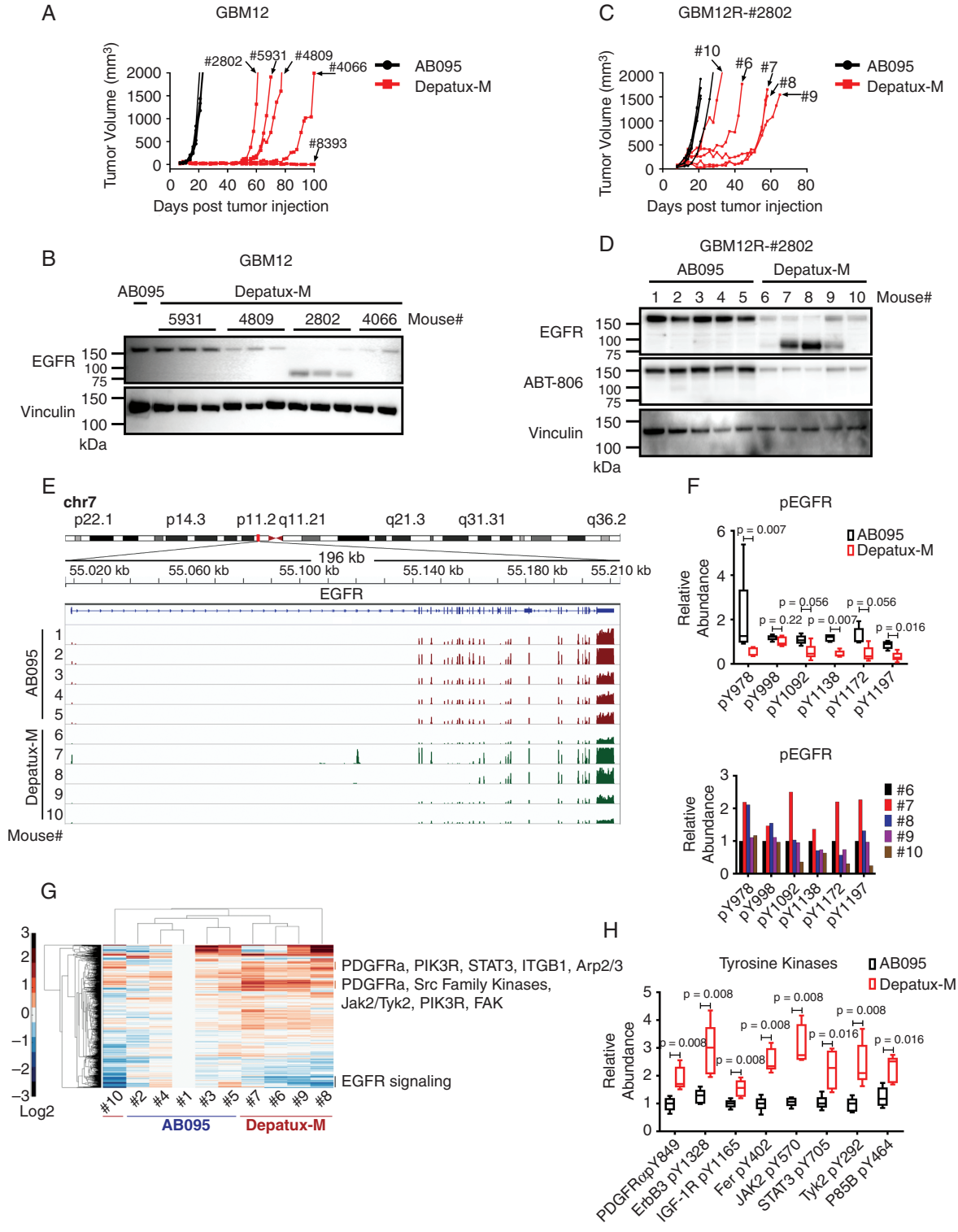

Fig. 2 Modulated EGFR expression imparts resistance to Depatux-M therapy in recurrent GBM12 PDX line. (A) Recurrent tumor growth of GBM12 PDX after AB095 (5 mg/kg) and Depatux-M (5 mg/kg) therapy. Four-digit numbers denote a truncated animal ID#. Data is from the same experiment shown in Figure 1D for GBM12. (B) EGFR expression in AB095-treated and serially passaged recurrent Depatux-M treated tumors derived from GBM12. Vinculin was used as a loading control. (C) Tumor growth of GBM12R-#2802 subline in the flank of mice treated with weekly intraperitoneal injections of AB095 (5 mg/kg) and Depatux-M (5 mg/kg). Single digit number corresponds to individual mice/tumors analyzed subsequently. (D) EGFR expression detected by anti-EGFR and ABT-806 antibody in the lysates from AB095 and Depatux-M treated GBM12R-#2802 tumors. Vinculin

but not all, of the GBM12R-#2802 and GBM12R-#5931 Depatux-M-treated tumors (Figure 2D and Supplementary Figure 3B). This short-variant was not recognized using the ABT-806 antibody, consistent with deletion in the extracellular domain that contains the antibody epitope (Figure 2D). Interestingly, levels of extrachromosomal EGFR gene copies measured by FISH were only suppressed in those tumors with suppression of full-length EGFR (Mouse #6, 9, and 10; Supplementary Figure 3C).

RNAseq of AB095 and Depatux-M-recurrent tumors from the GBM12R-#2802 experiment was used to further characterize these recurrent tumors. Similar to the FISH analysis, only recurrent tumors (#6, 9, 10) with full-length EGFR had significantly lower abundance of EGFR transcript (P = .025) (Supplementary Figure 3D). In an analysis of exon usage across the Depatux-M-treated tumors, mRNA representation of exons 5–12 were suppressed in both tumors #7 and #8 expressing the short-variant EGFR. These exons encode for the translated C-terminal portion of CR1 and L2 extracellular domains of EGFR protein containing Depatux-M binding epitope (Supplementary Table 2, Figure 2E, and Supplementary Figure 3E). Coupled with the variable re-emergence of the short-variant in the GBM12R-#2802 and GBM12R-#5931 sublines, these data suggest a highly plastic mechanism possibly involving genomic deletion variants of EGFR extrachromosomal DNA or differential exon splicing in the setting of Depatux-M selection pressure.

The impact of Depatux-M selection in GBM12R-#2802 treated tumors also was analyzed by global phosphotyrosine proteomic analysis. There was an overall reduction in the phosphorylation of EGFR at multiple sites in Depatux-M recurrent tumors (mice #6–10); however, EGFR phosphorylated peptides were detected at higher levels in the tumors with short-variant (#7, 8) as compared to other Depatux-M treated tumors (Figure 2F). Further analysis beyond EGFR demonstrated upregulation in Depatux-M-treated tumors of multiple phosphotyrosine sites in kinase signaling pathways implicated in resistance to EGFR inhibitors (Figure 2G and H, Supplementary Figure 3F and G, Supplementary Tables 3 and 4). Collectively, these data suggest heightened compensatory signaling pathways contribute to the Depatux-M-resistance phenotype in GBM12R tumors.

BBB Integrity Affects the Efficacy of Depatux-M in Orthotopic PDXs

The efficacy of Depatux-M in six sensitive GBM PDX models was evaluated in orthotopic tumors. Given the generally limited efficacy of ABT-806 and/or AB095-MMAF in the heterotopic tumors, these controls were not included. In contrast to flank studies, response to Depatux-M therapy across PDXs in intracranial models was highly heterogeneous. GBM39 and GBM84 remained highly responsive to therapy with continuous suppression of BLI signal to background and an increase in median survival of 289 and 192 days, respectively, compared to control (Figure 3A and B, Supplementary Figure 4A). In contrast, GBM6 was resistant to therapy, without detectable impact on tumor growth and a statistically significant but nominal 5-day increase in median survival (Figure 3A and B; P = .003). GBM12, GBM76, and GBM26 had a similarly limited response, with a median survival extension of 15, 19, and 13 days, respectively (Figure 3A and B, Supplementary Figure 4B; Supplementary Table 5). Thus, in contrast to impressive and near-uniform activity of Depatux-M across flank tumors, only two of the PDXs were highly responsive to Depatux-M as orthotopic tumors.

Depatux-M delivery relative to drug efficacy was evaluated in mice with orthotopic GBM6 and GBM39 tumors. Mice were dosed with Depatux-M and subsequently, fixed brains were sectioned and processed for coimmunofluorescence to detect human tumor cells (antihuman Lamin A/C), Depatux-M accumulation (antihuman IgG), and BBB disruption (murine fibrinogen). GBM39 exhibited readily detectable Depatux-M accumulation and significant fibrinogen extravasation in the tumor region. In contrast, GBM6 had minimal accumulation of Depatux-M in tumor and no detectable fibrinogen accumulation (Figure 3C). Consistent with physical disruption of the BBB, fibrinogen accumulation in GBM39 tumors was associated with disruption of endothelial tight-junctions, as evidenced by discontinuous claudin-5 staining. In contrast, continuous, uninterrupted claudin-5 staining of brain tumor capillaries and absence of fibrinogen accumulation were observed in GBM6. (Supplementary Figure 4C). Differences in toxin delivery were analyzed by matrix-assisted laser desorption/ionization mass spectrometry imaging (MALDI-MSI). Forty-eight hours after Depatux-M dosing, the average Cys-mc-MMAF concentration was 2.93 ± 1.53 μM in GBM39, while Cys-mc-MMAF concentrations were below the limit of quantitation for all but one AB095-MMAF treated GBM39 samples and for all GBM6 samples (Figure 3D and Supplementary Figure 5A, B, and C). Collectively, these data suggest that Depatux-M is highly effective for EGFR-amplified GBM, but that efficacy might be limited by poor drug delivery across the BBB.

Enhanced Depatux-M Delivery Into Orthotopic Tumors Increases Treatment Eficacy

The comparison of GBM6 and GBM39 suggests that BBB disruption may be important for Depatux-M efficacy. To test this, we used a previously described PDX model of BBB disruption: GBM108 expressing vascular endothelial

was used as a loading control. (E) EGFR gene exon usage with differential expression in AB095 and Depatux-M treated GBM12R-#2802 tumors as assessed by RNAseq analysis. (F) Relative abundance of phosphopeptides of EGFR in AB095 and Depatux-M treated mice, and graph below shows relative levels in individual Depatux-M treated mice. (G) Heat map with relative levels of phosphopeptides after Depatux-M treatment of GBM12R-#2802 subline as detected by phosphotyrosine proteomics analysis. (H) Relative abundance of phosphopeptides from tyrosine kinases; PDGFRα, ErbB3, IGF-1R, Fer, JAK2, STAT3, TYK2 and P85B following AB095 and Depatux-M treatment. Significance between AB095 and Depatux-M treated groups in F and H was calculated using Mann–Whitney test.

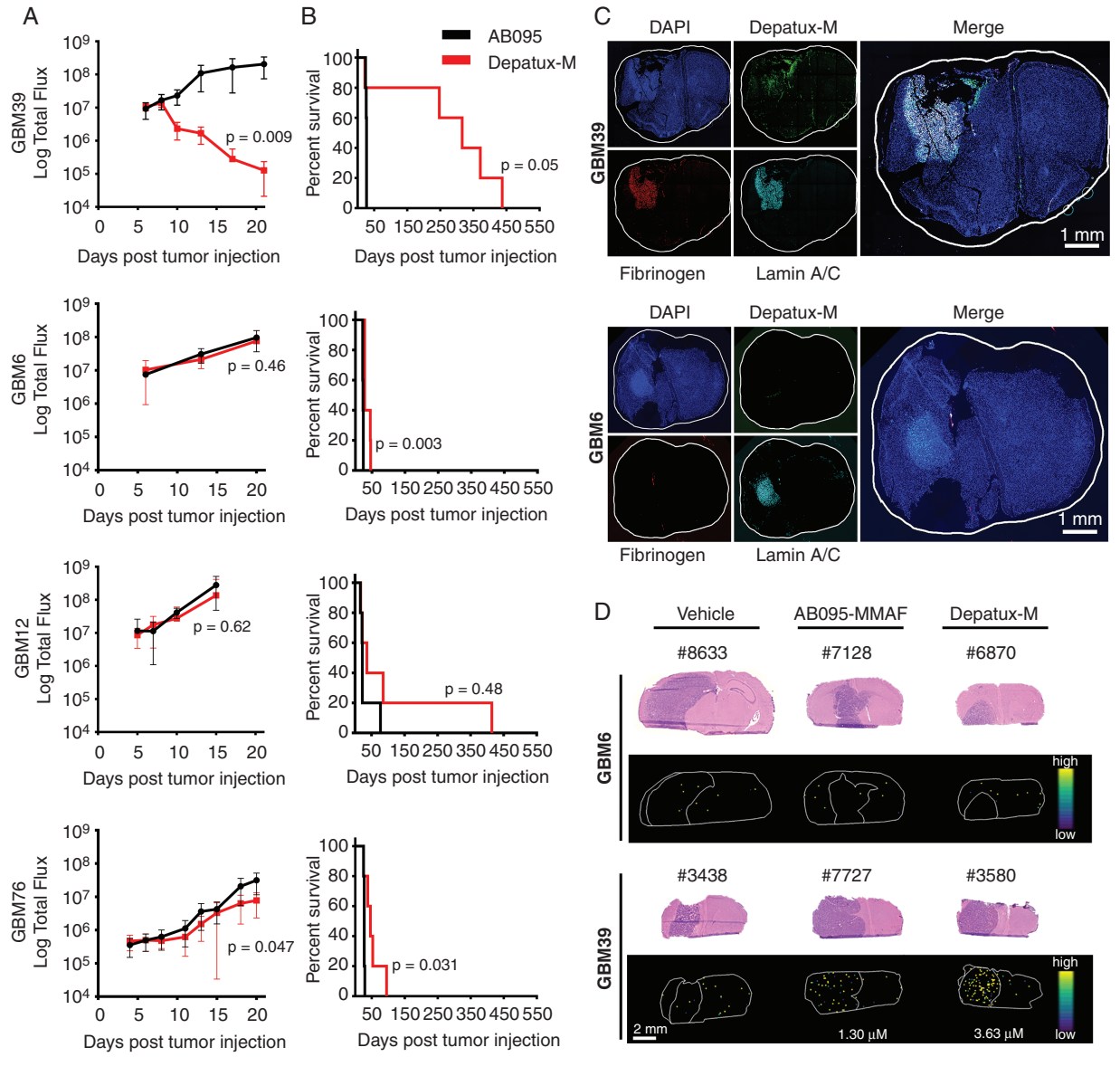

Fig. 3. Depatux-M intracranial efficacy is limited due to poor delivery across blood-brain barrier. (A-B) Intracranial tumor growth of indicated PDXs, as measured by bioluminescence imaging (BLI) (A) and Kaplan–Meier curves showing time to reach moribund state after weekly intraperitoneal AB095 (5 mg/kg) or Depatux-M (5 mg/kg) treatment for up to 6 months (B) with exception of GBM39, which was dosed weekly for 400 days. Data are presented as means ± SEM and significance between treated groups was calculated for the last data point using Kruskal–Wallis test in A. Significance of endpoint comparison between Depatux-M and AB095 group is shown using Log-Rank test in B. (C) Uptake of Depatux-M and integrity of blood-brain barrier as measured by fibrinogen staining in GBM39 and GBM6 intracranial tumors by immunofluorescence microscopy. Antihuman Lamin A/C was used to stain tumor cells in brain. Results are representative of 3 animals for each PDX. (D) Ion images of brain tissue sections from representative AB095-MMAF (5 mg/kg) and Depatux-M (5 mg/kg) treated animals with either GBM6 or GBM39 orthotopic tumors after a single intraperitoneal dose with corresponding H&E microscopy images. Ion images reflect the spatial distribution of the Cys-mc-MMAF fragment used for quantitation.

growth factor-A (GBM108VEGF) or an empty vector (GBM108EV).[12] Orthotopic GBM108VEGF was highly responsive to Depatux-M with significant reduction in BLI signal and increase in median survival of 222 days compared to 30.5 days for AB095 control (Figure 4A and B; *P* = .040). In contrast, GBM108EV was poorly responsive to therapy, with limited impact on tumor growth as measured by BLI and a median extension in survival of only 30 days (*P* = .004; Supplementary Table 6). Similar to the studies above, GBM108VEGF showed significant staining for fibrinogen and enhanced Depatux-M accumulation compared to GBM108EV (Figure 4C). Consistent with fibrinogen accumulation within brain tumor tissue associated with BBB disruption, GBM108VEGF tumors

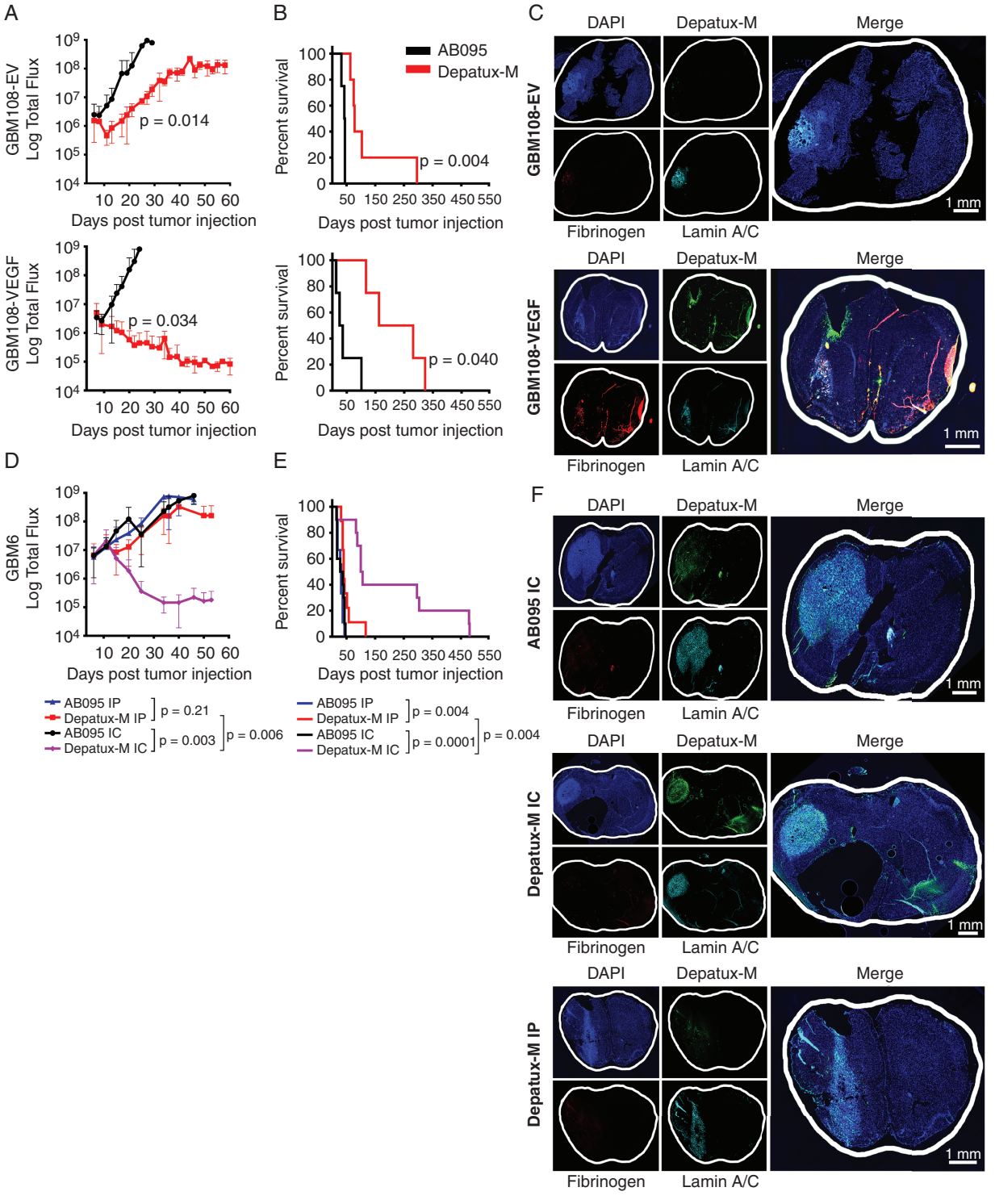

Fig. 4 Increased intracranial concentration of Depatux-M significantly enhances its efficacy. (A–B) Growth of orthotopic GBM108-EV and GBM108-VEGF tumors, as measured by BLI, after treatment with weekly intraperitoneal dose of 5 mg/kg of either AB095 or Depatux-M for up to 6 months (A) and Kaplan–Meier curves showing time to reach moribund state after treatment (B). (C) Depatux-M uptake and fibrinogen accumulation in the GBM108-EV and GBM108-VEGF brain sections using immunofluorescence microscopy. Results are representative of two mice in each group. (D–E) Intracranial tumor growth by BLI (D) and Kaplan–Meier survival curves (E) for mice with orthotopic GBM6 tumors treated with 4 total doses of AB095 or Depatux-M given weekly either intraperitoneally (IP) or intracranially (IC). (F) Immunofluorescence imaging of fibrinogen and Depatux-M in GBM6 intracranial tumors treated IP or IC with AB095 or Depatux-M. Antihuman Lamin A/C was used to stain human PDX cells in brain. Results are representative of two mice in each group. BLI data are presented as means ± SEM, and significance between groups was calculated using Kruskal–Wallis test. Significance of endpoint comparison between treatment groups for either IP or IC therapy are calculated using Log-Rank test.

exhibited activation of resident microglia[13,14] as compared to GBM6 and GBM26 tumors (Supplementary Figure 4D). Although manipulation of VEGF expression is not clinically feasible, these data demonstrate that enhanced delivery associated with BBB disruption can increase the efficacy of Depatux-M.

Multiple signaling pathways can influence BBB disruption, and an exploratory evaluation was performed in relation to the PDXs tested. Basal levels of VEGFA, assessed by Western blot in heterotopic tumors and by RNAseq in orthotopic tumors, did not correlate with orthotopic response to Depatux-M (Supplementary Figure 4E). Further, analysis of RNAseq data from orthotopic PDXs did not identify correlations of Depatux-M response and Olig2, Plasmalemma Vesicle Associated Protein (Plvap), Wnt7, or p53 loss, which has been previously associated with fibrinogen accumulation and BBB disruption.[15] Similarly, no correlation with treatment efficacy was observed in relationship to GBM molecular subtype or other phenotype markers, such as Sox2, Sox9, or Olig2 (data not shown and Supplementary Figure 4F).

Direct intratumoral drug injection by convection-enhanced delivery is a clinically relevant strategy that can be used to bypass the BBB and enhance delivery of large biomolecules. Therefore, the efficacy of direct intracranial Depatux-M injection into orthotopic GBM6 tumors was compared to systemic delivery. Strikingly, intracranial Depatux-M therapy resulted in a 3.5 log reduction in BLI signal compared to AB095 control, while BLI signal with intraperitoneal Depatux-M therapy was no different than control (Figure 4D). Serial intracranial Depatux-M injections resulted in a 71-day extension in median survival compared to AB095 intracranial injection ($P = .0001$), while serial intraperitoneal Depatux-M treatment nominally extended survival (10-day extension; $P = .06$) (Figure 4E). Consistent with effective bypass of the BBB, Depatux-M, but not AB095, was readily detectable by coimmunofluorescence 24 h after direct intracranial injection into orthotopic GBM6 tumors (Figure 4F). In contrast, systemic dosing was associated with minimal accumulation of ADC (Figure 4F). Collectively, these data provide direct evidence that enhanced delivery to GBM tumors can significantly increase the efficacy of Depatux-M.

Discussion

Antibody drug conjugates can deliver highly toxic payloads specifically to tumor cells, while sparing normal tissues. Almost half of GBM are driven by oncogenic genomic EGFR amplification, mutations, and exon splicing variants,[16–18] and those tumors with high-level EGFR expression are expected to be highly sensitive to Depatux-M. Unfortunately, two large randomized clinical trials in EGFR-amplified GBM patients failed to demonstrate a survival benefit for Depatux-M therapy in patients with newly diagnosed (Intellance-I) or recurrent (Intellance-II) disease.[8,19] In the current study, the profound antitumor benefit observed in nine of ten EGFR-amplified heterotopic GBM PDXs confirms a tremendous therapeutic potential for EGFR-targeted ADCs, but the heterogeneous activity and delivery in orthotopic tumors highlights the influence of the brain microenvironment on limiting the efficacy of Depatux-M in GBM.

A fundamental premise of modern oncology is that delivery of a minimally efficacious concentration of cytotoxic therapy throughout a tumor volume is required to provide a chance for cure, and the corollary is that inadequate delivery to a significant portion of a tumor can lead to rapid recurrence. Beyond the integrity of the BBB, efficient delivery of drugs into brain tumors can be adversely affected by multiple other mechanisms, including elevated interstitial fluid pressure, regions of poor vascularity, and limited vascular perfusion.[20,21] In this context, Depatux-M accumulation after systemic dosing was very low in orthotopic GBM6 (Figure 3) and GBM108EV (Figure 4) tumors, and associated with a lack of efficacy, while accumulation and efficacy in GBM39 or GBM108VEGF was much greater. These latter tumors both have a more disrupted BBB associated with aberrant accumulation of fibrinogen (340 kDa) that is normally confined to the vascular space. As expected, artificial disruption of the BBB through overexpression of VEGF in the GBM108VEGF tumors was associated with both enhanced accumulation of Depatux-M and a marked survival benefit. Although the BBB integrity was not specifically interrogated across all orthotopic PDXs and we did not observe a correlation between Depatux-M efficacy and endogenous VEGFA expression or signaling, we anticipate that limited drug distribution similarly limits Depatux-M delivery and efficacy across the models tested.

The marked enhancement in survival associated with direct intratumoral injection of Depatux-M into orthotopic GBM6 tumors is consistent with drug delivery being a fundamental resistance mechanism. Essentially all human GBM have regions of tumor cells with a relatively intact BBB, as evidence by heterogeneous contrast accumulation in regions of bulk tumor.[22] This suggests that heterogeneous delivery of Depatux-M could have been a major contributing factor to the lack of efficacy observed in clinical trials. Similar mechanisms likely limit accumulation of other large bio-molecules, such as immunotoxins, nanoparticles, and viruses, to regions with an intact BBB. Further, anti-VEGF therapies like bevacizumab can normalize the BBB, as evidenced by relatively rapid reduction in contrast enhancement in a subset of GBM patients. These observations suggest that combinations of antiangiogenic therapies with large biomolecules may limit delivery and efficacy of the latter therapeutics. Thus, defining the impact of heterogeneous ADC distribution within GBM patients is critically important for guiding clinical development for a number of novel therapeutic strategies. While careful image-guided intrapatient sampling in the context of Phase 0 surgical studies ultimately will be required to confirm our hypothesis, the data presented strongly suggest that drug delivery across the BBB should be a critical consideration when translating promising large biomolecular therapies into clinical testing for GBM.

There are additional mechanisms of resistance that likely contributed to the clinical failure of Depatux-M in GBM. GBM59 was inherently resistant to Depatux-M *in vivo*, though highly sensitive *in vitro*, but we were unable to define the mechanism underpinning this effect. In GBM12 and GBM46 *in vitro* uptake of Depatux-M was limited, consistent with a lower cell surface expression of EGFR as

compared to other EGFR-expressing cells. In these models, recurrent tumors exhibited overall suppression of EGFR or expression of an EGFR variant lacking the binding epitope for Depatux-M. Loss of EGFR-Depatux-M binding at the cell surface will limit internalization and prevent toxin release from the ADC and is consistent with known mechanisms of resistance to HER2-targeted ADCs.[23] Compensatory signaling associated with altered EGFR expression also was detected in models of acquired resistance to Depatux-M in GBM12 sublines with elevated signaling of several mitogenic signaling pathways (PDGFRA, JAK/STAT, and Src family kinases) known to function in parallel or downstream from EGFR.[24,25] While this is the first report of mechanisms of resistance to EGFR ADCs, similar compensatory signaling through EGFR, STAT3 and YES are known mechanisms of resistance to HER2-targeted T-DM1 ADC in HER2-amplified breast cancer models.[26–28] The emergence of a short-variant EGFR with apparent intact C-terminal tyrosine phosphorylation and downstream signaling likely reflects differential exon usage resulting in deletion of the CR1 domain, which includes the epitope for the ABT-806/Depatux-M. Although this variant has not been reported previously in GBM, evolution of a similar truncated HER2 molecule lacking an extracellular domain but with retained downstream signaling was reported in association with resistance to HER2-targeted antibodies and ADCs.[29] Although more detailed molecular mechanistic studies are required, our data are consistent with alternative splicing or extrachromosomal DNA genomic deletions that result in a functional EGFR molecule that is insensitive to Depatux-M, although the highly plastic nature of this event has made studying this phenomenon especially challenging.

The clinical rationale for developing ADCs for solid tumors with high-level receptor tyrosine kinase expression is provided by the impressive results with HER2-targeted ADCs in breast cancer.[30] Although HER2-targeted antibodies have limited activity in brain metastases, multiple studies have demonstrated significant clinical benefit with T-DM1 therapy in patients with clinically evident brain metastases.[31,32] These data are consistent with distribution of at least a minimally-efficacious concentration of T-DM1 into these brain metastases, which are typically more homogeneously enhancing and much less invasive than GBM. However, in two large prospective studies evaluating T-DM1 therapy in locally advanced/metastatic (KAMILLA) or early stage (KATHERINE) HER2+ breast cancer, there was a high rate of new brain metastasis development while on T-DM1 therapy.[32,33] These data are consistent with the concept that small foci of micrometastatic disease in the brain have an intact BBB and are not adequately treated by large ADC biomolecules. This context of tumor targets being "protected" by the BBB is analogous to noncontrast enhancing regions of GBM with a relatively intact BBB and further reiterates the importance of adequate drug delivery to all sites of tumor burden.

There are important limitations to the present study. First, although GBM PDXs closely reflect the genomics of the originating human tumor,[9] they likely display less molecular heterogeneity than human GBM. Similarly, orthotopic PDXs in mice are an order of magnitude smaller than human GBM and undoubtedly have much less heterogeneity in BBB disruption and other aspects of tumor biology dependent on the tumor microenvironment. Importantly, ADC-mediated cell killing can evoke antitumor immune responses that cannot be modeled in the immuno-deficient mice used in this study.[34–36] Nonetheless, the studies performed demonstrate that EGFR-targeting ADCs are potent cytotoxic agents with a significant potential for antitumor efficacy in GBM. While the results from the Intellance I and II clinical trials with Depatux-M in GBM were clearly disappointing, our results provide a strong impetus to redouble our efforts to investigate novel strategies to enhance ADC delivery across the BBB to more effectively treat this devastating disease.

Supplementary Material

Supplementary data are available at *Neuro-Oncology* online.

Keywords

antibody drug conjugates | blood-brain barrier | Depatux-M | EGFR | glioblastoma

Funding

Funding was provided by the MIT/Mayo Physical Sciences Center for Drug Distribution and Efficacy in Brain Tumors U54 CA210180 (J.N.S., F.M.W., N.Y.R.A., J.R.C., W.F.E.); Mayo Clinic; NIH T32EB025823 (S.A.S.) fellowship in partnership with the Ferenc Jolesz National Center for Image Guided Therapy at Brigham and Women's Hospital (P41 EB015898). M.H.M. received an NSF GRFP Fellowship.

Acknowledgments

AB095, AB095-MMAF, ABT-806, and Depatux-M (ABT-414) were provided by AbbVie Inc. We appreciate the detailed guidance and careful manuscript review by Vincent Blot and Edward Reilly from AbbVie Inc. We are grateful to Mayo Cytogenetics Core facility for FISH assay and analysis. We thank Dr. Aaron Johnson and Fang Jin for help and guidance with claudin-5 staining.

Authorship statement. N.Y.R.A., W.F.E., F.M.W., J.N.S. worked on the conceptualization. B.M.M., K.A.P., S.J., M.K., A.C.M., C.L.M., J.E.C.-P., J.-H.O., S.T., D.M.B., R.A.V., C.G., S.T., S.K.G., L.H., B.L.C., K.B., M.H.M., S.A.S., M.S.R., T.C.B., I.F.P., P.A.D., J.E.E-P. performed the experiments. B.-M.M., K.A.P., S.J., C.L.M., J.E.C.-P., R.A.V., C.G., M.H.M., S.A.S., M.S.R., N.Y.R.A., G.J.K., S.T., D.M.B., P.A.D., J.E.E.-P., J.R.C., W.F.E., F.M.W., J.N.S. performed the data analysis. K.A.P., S.J., F.M.W., J.N.S., N.Y.R.A. were involved in manuscript writing.

Conflict of interests statement. While these studies were not funded by AbbVie Inc., AbbVie Inc. provided research funding to the Sarkaria laboratory in August 2020 for follow-on studies. In compliance with Harvard Medical School and Partners Healthcare guidelines on potential conflict of interest, we disclose that N.Y.R.A. is scientific advisor to BayesianDx.

References

1. Weiner LM, Surana R, Wang S. Monoclonal antibodies: versatile platforms for cancer immunotherapy. *Nat Rev Immunol.* 2010;10(5):317–327.
2. Furnari FB, Cloughesy TF, Cavenee WK, Mischel PS. Heterogeneity of epidermal growth factor receptor signalling networks in glioblastoma. *Nat Rev Cancer.* 2015;15(5):302–310.
3. Phillips AC, Boghaert ER, Vaidya KS, et al. ABT-414, an antibody-drug conjugate targeting a tumor-selective EGFR epitope. *Mol Cancer Ther.* 2016;15(4):661–669.
4. Jungbluth AA, Stockert E, Huang HJ, et al. A monoclonal antibody recognizing human cancers with amplification/overexpression of the human epidermal growth factor receptor. *Proc Natl Acad Sci U S A.* 2003;100(2):639–644.
5. Reilly EB, Phillips AC, Buchanan FG, et al. Characterization of ABT-806, a humanized tumor-specific anti-EGFR monoclonal antibody. *Mol Cancer Ther.* 2015;14(5):1141–1151.
6. Chen H, Lin Z, Arnst KE, Miller DD, Li W. Tubulin inhibitor-based antibody-drug conjugates for cancer therapy. *Molecules.*. 2017;22(8):1281.
7. van den Bent M, Gan HK, Lassman AB, et al. Efficacy of depatuxizumab mafodotin (ABT-414) monotherapy in patients with EGFR-amplified, recurrent glioblastoma: results from a multi-center, international study. *Cancer Chemother Pharmacol.* 2017;80(6):1209–1217.
8. Lassman A, Pugh S, Wang T, et al. ACTR-21. A randomized, double-blind, placebo-controlled Phase 3 trial of depatuxizumab mafodotin (ABT-414) in epidermal growth factor receptor (EGFR) amplified newly diagnosed glioblastoma (nGBM). *Neuro Oncol.* 2019;21(Supplement_6):vi17.
9. Vaubel RA, Tian S, Remonde D, et al. Genomic and phenotypic characterization of a broad panel of patient-derived xenografts reflects the diversity of glioblastoma. *Clin Cancer Res.* 2020;26(5):1094–1104.
10. Carlson BL, Pokorny JL, Schroeder MA, Sarkaria JN. Establishment, maintenance and in vitro and in vivo applications of primary human glioblastoma multiforme (GBM) xenograft models for translational biology studies and drug discovery. *Curr Protoc Pharmacol.* 2011;Chapter 14(14):Unit 14.16.
11. Wang XQ, Sun P, O'Gorman M, Tai T, Paller AS. Epidermal growth factor receptor glycosylation is required for ganglioside GM3 binding and GM3-mediated suppression [correction of suppresion] of activation. *Glycobiology.* 2001;11(7):515–522.
12. Kim M, Ma DJ, Calligaris D, et al. Efficacy of the MDM2 inhibitor SAR405838 in glioblastoma is limited by poor distribution across the blood-brain barrier. *Mol Cancer Ther.* 2018;17(9):1893–1901.
13. Petersen MA, Ryu JK, Chang KJ, et al. Fibrinogen activates BMP signaling in oligodendrocyte progenitor cells and inhibits remyelination after vascular damage. *Neuron.* 2017;96(5):1003–1012.e7.
14. Bardehle S, Rafalski VA, Akassoglou K. Breaking boundaries-coagulation and fibrinolysis at the neurovascular interface. *Front Cell Neurosci.* 2015;9:354.
15. Griveau A, Seano G, Shelton SJ, et al. A glial signature and wnt7 signaling regulate glioma-vascular interactions and tumor microenvironment. *Cancer Cell.* 2018;33(5):874–889 e877.
16. Gan HK, Kaye AH, Luwor RB. The EGFRvIII variant in glioblastoma multiforme. *J Clin Neurosci.* 2009;16(6):748–754.
17. Aldape KD, Ballman K, Furth A, et al. Immunohistochemical detection of EGFRvIII in high malignancy grade astrocytomas and evaluation of prognostic significance. *J Neuropathol Exp Neurol.* 2004;63(7):700–707.
18. Cloughesy TF, Cavenee WK, Mischel PS. Glioblastoma: from molecular pathology to targeted treatment. *Annu Rev Pathol.* 2014;9:1–25.
19. Van Den Bent M, Eoli M, Sepulveda JM, et al. INTELLANCE 2/ EORTC 1410 randomized phase II study of Depatux-M alone and with temozolomide vs temozolomide or lomustine in recurrent EGFR amplified glioblastoma. *Neuro Oncol.* 2020;22(5):684–693.
20. Persson AI, Ilkhanizadeh S, Miroshnikova YA, et al. High interstitial fluid pressure regulates tumor growth and drug uptake in human glioblastoma. *Neuro Oncol.* 2014;16(Suppl 3):iii32.
21. Lunt SJ, Fyles A, Hill RP, Milosevic M. Interstitial fluid pressure in tumors: therapeutic barrier and biomarker of angiogenesis. *Future Oncol.* 2008;4(6):793–802.
22. Sarkaria JN, Hu LS, Parney IF, et al. Is the blood-brain barrier really disrupted in all glioblastomas? A critical assessment of existing clinical data. *Neuro Oncol.* 2018;20(2):184–191.
23. Li G, Guo J, Shen BQ, et al. Mechanisms of acquired resistance to trastuzumab emtansine in breast cancer cells. *Mol Cancer Ther.* 2018;17(7):1441–1453.
24. Seshacharyulu P, Ponnusamy MP, Haridas D, Jain M, Ganti AK, Batra SK. Targeting the EGFR signaling pathway in cancer therapy. *Expert Opin Ther Targets.* 2012;16(1):15–31.
25. Saleem H, Kulsoom Abdul U, Kucukosmanoglu A, et al. The TICking clock of EGFR therapy resistance in glioblastoma: target independence or target compensation. *Drug Resist Updat.* 2019;43:29–37.
26. Endo Y, Shen Y, Youssef LA, Mohan N, Wu WJ. T-DM1-resistant cells gain high invasive activity via EGFR and integrin cooperated pathways. *MAbs.* 2018;10(7):1003–1017.
27. Wang L, Wang Q, Gao M, et al. STAT3 activation confers trastuzumab-emtansine (T-DM1) resistance in HER2-positive breast cancer. *Cancer Sci.* 2018;109(10):3305–3315.
28. Wang L, Wang Q, Xu P, et al. YES1 amplification confers trastuzumab-emtansine (T-DM1) resistance in HER2-positive cancer. *Br J Cancer.* 2020;123(6):1000–1011.
29. Ward TM, Iorns E, Liu X, et al. Truncated p110 ERBB2 induces mammary epithelial cell migration, invasion and orthotopic xenograft formation, and is associated with loss of phosphorylated STAT5. *Oncogene.* 2013;32(19):2463–2474.
30. Kunte S, Abraham J, Montero AJ. Novel HER2-targeted therapies for HER2-positive metastatic breast cancer. *Cancer.* 2020;126(19):4278–4288.
31. Jacot W, Pons E, Frenel JS, et al. Efficacy and safety of trastuzumab emtansine (T-DM1) in patients with HER2-positive breast cancer with brain metastases. *Breast Cancer Res Treat.* 2016;157(2):307–318.
32. Montemurro F, Delaloge S, Barrios CH, et al. Trastuzumab emtansine (T-DM1) in patients with HER2-positive metastatic breast cancer and brain metastases: exploratory final analysis of cohort 1 from KAMILLA, a single-arm phase IIIb clinical trial. *Ann Oncol.* 2020;31(10):1350–1358.

33. von Minckwitz G, Huang CS, Mano MS, et al.; KATHERINE Investigators. Trastuzumab emtansine for residual invasive HER2-positive breast cancer. *N Engl J Med*. 2018;380(7):617–628.
34. Rios-Doria J, Harper J, Rothstein R, et al. Antibody-drug conjugates bearing pyrrolobenzodiazepine or tubulysin payloads are immunomodulatory and synergize with multiple immunotherapies. *Cancer Res*. 2017;77(10):2686–2698.
35. Gerber HP, Sapra P, Loganzo F, May C. Combining antibody-drug conjugates and immune-mediated cancer therapy: what to expect? *Biochem Pharmacol*. 2016;102:1–6.
36. D'Amico L, Menzel U, Prummer M, et al. A novel anti-HER2 anthracycline-based antibody-drug conjugate induces adaptive anti-tumor immunity and potentiates PD-1 blockade in breast cancer. *J ImmunoTher Cancer*. 2019;7(1):16.